The Astrophysical Journal, 823:9 (7pp), 2016 May 20 doi:10.3847/0004-637X/823/1/9

THE ACS LCID PROJECT. XI. ON THE EARLY TIME RESOLUTION OF SFHs OF LOCAL GROUP DWARF GALAXIES: COMPARING THE EFFECTS OF REIONIZATION IN MODELS WITH OBSERVATIONS*

Antonio Aparicio[1,2], Sebastian L. Hidalgo[1,2], Evan Skillman[3], Santi Cassisi[1,4], Lucio Mayer[5,6], Julio Navarro[7], Andrew Cole[8], Carme Gallart[1,2], Matteo Monelli[1,2], Daniel Weisz[9,10,14], Edouard Bernard[11], Andrew Dolphin[12], and Peter Stetson[13]

[1] Instituto de Astrofísica de Canarias, Vía Láctea s/n, E38200—La Laguna, Tenerife, Canary Islands, Spain; aaj@iac.es, shidalgo@iac.es, carme@iac.es, monelli@iac.es
[2] Department of Astrophysics, University of La Laguna, Vía Láctea s/n, E38200—La Laguna, Tenerife, Canary Islands, Spain
[3] INAF–Osservatorio Astronomico di Collurania, Teramo, Italy; cassisi@oa-teramo.inaf.it
[4] Intitut für Theoretische Physics, University of Zurich, Zürich, Switzerland; lucio@physics.unizh.ch
[5] Department of Physics, Institut für Astronomie, ETH Zürich, Zürich, Switzerland; lucio@phys.ethz.ch
[6] Department of Physics and Astronomy, University of Victoria, BC V8P 5C2, Canada; jfn@uvic.ca
[7] Minnesota Institute for Astrophysics, University of Minnesota, Minneapolis, MN 55455, USA; skillman@astro.umn.edu
[8] School of Physical Sciences, University of Tasmania, Hobart, Tasmania, Australia; andrew.cole@utas.edu.au
[9] Astronomy Department, Box 351580, University of Washington, Seattle, WA 92895, USA; dweisz@uw.edu
[10] Department of Astronomy, University of California at Santa Cruz, 1156 High Street, Santa Cruz, CA 95064, USA
[11] Institute for Astronomy, University of Edinburgh, Royal Observatory, Blackford Hill, Edinburgh EH9 3HJ, UK; ejb@roe.ac.uk
[12] Raytheon, 1151 East Hermans Road, Tucson, AZ 85706, USA; adolphin@raytheon.com
[13] Dominion Astrophysical Observatory, Herzberg Institute of Astrophysics, National Research Council, 5071 West Saanich Road, Victoria, BC V9E 2E7, Canada; peter.stetson@nrc-cnrc.gc.ca
Received 2015 June 23; accepted 2016 March 16; published 2016 May 16

ABSTRACT

The analysis of the early star formation history (SFH) of nearby galaxies, obtained from their resolved stellar populations, is relevant as a test for cosmological models. However, the early time resolution of observationally derived SFHs is limited by several factors. Thus, direct comparison of observationally derived SFHs with those derived from theoretical models of galaxy formation is potentially biased. Here we investigate and quantify this effect. For this purpose, we analyze the duration of the early star formation activity in a sample of four Local Group dwarf galaxies and test whether they are consistent with being true fossils of the pre-reionization era; i.e., if the quenching of their star formation occurred before cosmic reionization by UV photons was completed. Two classical dSph (Cetus and Tucana) and two dTrans (LGS-3 and Phoenix) isolated galaxies with total stellar masses between 1.3×10^6 and 7.2×10^6 $M_\odot$ have been studied. Accounting for time resolution effects, the SFHs peak as much as 1.25 Gyr earlier than the optimal solutions. Thus, this effect is important for a proper comparison of model and observed SFHs. It is also shown that none of the analyzed galaxies can be considered a true fossil of the pre-reionization era, although it is possible that the *outer regions* of Cetus and Tucana are consistent with quenching by reionization.

Key words: early universe – galaxies: dwarf – galaxies: evolution – galaxies: photometry – galaxies: stellar content – galaxies: structure

1. INTRODUCTION

Dwarf galaxies are at the focus of a major cosmological problem affecting the ΛCDM scenario: the number of dark matter subhalos around Milky Way-type galaxies predicted by ΛCDM simulations is much larger than the number of observed satellite dwarf galaxies (Kauffmann et al. 1993; Klypin et al. 1999; Moore et al. 1999). Most proposals to overcome this problem stem from the idea that the smallest halos would have formed very few stars or failed to form stars at all, and that gas would have been removed in an early epoch. In this way, the subhalos with the lowest mass would be either completely dark, and thus undetectable, or extremely faint. Two main mechanisms are usually invoked as being responsible for the smallest subhalos failing to have an extended star formation history (SFH): heating from cosmic ultraviolet (UV) background radiation arising from the earliest star formation in the universe (Bullock et al. 2000) and internal supernova feedback (Mac Low & Ferrara 1999) following the first star formation episodes in the host dwarf galaxy. The cosmic UV background raises the entropy of the intergalactic medium around the epoch of reionization, preventing baryons from falling into the smallest subhalos, and it can also heat and evaporate the interstellar medium of larger subhalos that have managed some star formation. The former would never form stars while the latter would currently show only a very old stellar population (Mac Low & Ferrara 1999; Sawala et al. 2010; Shen et al. 2014; Benítez-Llambay et al. 2015). Recent high-resolution simulations of dwarf galaxy formation show that the cosmic UV radiation field can also still suppress star formation, even when it cannot evaporate the gas from the halos, by simply preventing gas from becoming dense enough to form molecular clouds (Shen et al. 2014), verifying a previous proposal by Schaye (2001).

It has also been proposed that ram pressure stripping in the diffuse corona of the host massive galaxy could very rapidly remove the interstellar medium already heated by the cosmic

* Based on observations made with the NASA/ESA *Hubble Space Telescope*, obtained at the Space Telescope Science Institute, which is operated by the Association of Universities for Research in Astronomy, Inc., under NASA contract NAS 5-26555. These observations are associated with program #10505.
[14] Hubble Fellow.

UV, even over a large range of dwarf galaxy masses (Mayer et al. 2007). However, such a mechanism would become dominant later, during the main accretion phase of a typical Milky Way-sized halo, at $z < 2$, in principle allowing star formation to extend for at least a couple of Gyr beyond the epoch of reionization.

Although consensus exists on the important role played by the two former mechanisms, less clear is the mass range of the affected subhalos (e.g., Gnedin 2000; Kravtsov et al. 2004; Shen et al. 2014; Benítez-Llambay et al. 2015). The fact that most or all of the recently discovered ultrafaint dwarfs (UFDs) appear to host only a small population of very old stars points to them as possible fossils of this process, but some of the classical dSph galaxies may also be affected. Besides heating the gas, UV photons produce the global cosmic reionization. The redshift at which the universe was fully reionized was $z \sim 6$, as obtained from the presence of the Gunn–Peterson trough in quasars (Becker et al. 2001; Loeb & Barkana 2001), although there is increasing evidence that this process was inhomogeneous (Spitler et al. 2012; Becker et al. 2015; Sobacchi & Mesinger 2015). According to models (see, e.g., Ricotti & Gnedin 2005; Gnedin & Kravtsov 2006; Bovill & Ricotti 2011a, 2011b), the minimum circular velocity for a dwarf halo to accrete and cool gas in order to produce star formation is in the range of $v_c \sim 20$–$30\,\mathrm{km\,s^{-1}}$, which corresponds to a total mass of $\sim 10^8$–$10^9\ M_\odot$. However, while most dwarf galaxies in the Local Group show circular velocities below this range and dynamical masses smaller than $\sim 10^8\ M_\odot$ (see, e.g., McConnachie 2012), many of them have color–magnitude diagrams (CMDs) that have been interpreted as indicating the presence of star formation activity extended well beyond the reionization epoch, even in old dSph galaxies (Grebel & Gallagher 2004; Monelli et al. 2010a, 2010b; Hidalgo et al. 2011; Weisz et al. 2014a, 2014b). Two main mechanisms have been proposed to overcome this problem. The first one is that dwarf halos could have been much larger in the past and have lost a significant amount of mass due to tidal harassment (Kazantzidis et al. 2004; Kravtsov et al. 2004). This scenario is further supported by detailed simulations of the tidal interaction between satellites and the host, which includes also the baryonic component and ram pressure stripping (Mayer et al. 2007; Mayer 2010). However, counter-arguments exists pointing to dwarf halos being resilient to tidal harassment (Peñarrubia et al. 2008). The second one is that a self-shielding mechanism would be at work, protecting the gas in the central denser regions of the dwarf galaxy, where gas can be optically thick to the impinging radiation field (Susa & Umemura 2004). The first mechanism is robust, since it is a natural consequence of hierarchical accretion as dwarf satellites move on highly eccentric orbits, suffering strong tidal shocks from the host potential. The second mechanism is more subtle, since models neglect a related, competitive effect, namely that the local UV radiation from the primary galaxy or nearby protoclusters could have been much higher than the mean cosmic ionizing flux at $z > 1$ (Mayer 2010; Iliev et al. 2011).

Models by Bovill & Ricotti (2011a, 2011b) show that Milky Way satellites with total luminosities $L_V > 10^6 L_\odot$ are very unlikely to be true fossils of the reionization epoch, and that they are probably the result of hierarchical build-up from smaller halos extending beyond the reionization epoch. More specifically, Bovill & Ricotti (2011a) conclude that the simulated properties of true fossils, i.e., those that have not undergone any merging events after reionization, agree with those of a subset of the UFD satellites of Andromeda and the Milky Way. Also, they found that most classical dSph satellites are unlikely true fossils, although they have properties in common with them: diffuse, old stellar populations and no gas. We note that, while it would seem natural to associate UFDs to reionization fossils, alternative explanations for their origin have recently appeared in the literature, in which at least a fraction of them could be remnants of the oldest, most heavily stripped population of galaxy satellites accreting at $z > 2$ onto the Milky Way halo (Tomozeiu et al. 2015).

Bovill & Ricotti (2011b) used the fraction of star formation produced before reionization as a test to distinguish true fossil galaxies from non-fossils, defining the former as those having produced at least 70% of their stars by $z = 6$. This criterion was defined after the analysis of the theoretical simulations and has the advantage of allowing a thorough comparison of models and observations. In turn, Weisz et al. (2014b) have obtained the SFHs of 38 Local Group dwarf galaxies with stellar masses in the range $10^4 < M_\star < 10^9 M_\odot$, finding that only five of them are consistent with forming the bulk of their stars before reionization and that only two out of the 13 true fossils predicted by Bovill & Ricotti (2011b) show a star formation quenched by reionization. However, it should be noted that the results of Weisz et al. (2014b) are affected by limited time resolution at early ages while the predictions by Bovill & Ricotti (2011b) are free of the these effects. These effects are expected to significantly modify the SFHs obtained from observational data, as can be seen in the simulations shown by, e.g., Hidalgo et al. (2011, 2013) among others. As a consequence of this, either observational effects should be simulated in theoretical models or they should be taken into consideration when comparing observational results with the theoretical models. The second is the objective of this paper.

In this paper, we discuss how the temporal resolution limitations of a SFH derived from a CMD might be accounted for. In particular, the goal of this paper is to obtain an estimate of the maximum fraction of mass, *consistent with the observations*, that has been converted into stars by $z = 6$ and of the time by which 70% of the baryonic mass has been converted into stars in each galaxy. These values can be directly compared with the predictions of any theoretical model of star formation in dwarf galaxies, and we do this comparison, for illustrative purposes, with some of the most recent ones currently available in the literature. We have used high-resolution SFHs obtained for a set of isolated Local Group dwarfs by the LCID collaboration (Hidalgo et al. 2013, and references therein). Our approach opens a new window to the possibility of testing the effects that cosmic UV radiation and internal supernova feedback have on the early SFH of dwarf galaxies (whether or not combined with self-shielding or other effects). This is an exploratory paper in which we provide details of the method and apply it to a sample of very well studied dwarf galaxies. Environmental effects, such as tides and ram pressure, affect the mappings between present-day and pre-infall mass of satellites and between baryon content and star formation. Therefore, we specifically concentrate on a sample of relatively isolated faint dwarfs. The chosen sample is diverse enough to contain dIrrs, transition dwarfs, and dSphs. In future works, the method will be applied to an extended sample including ultrafaint dwarfs.

Table 1
Summary of Data and Models

Galaxy/Model	M_* ($10^6 M_\odot$)	L_V ($10^6 L_\odot$)	σ_v (km s^{-1})	[Fe/H]
(1)	(2)	(3)	(4)	(5)
Cetus	7.17	2.58	17.0 ± 2.0	-1.9 ± 0.1
Tucana	1.66	0.54	$15.8^{+4.1}_{-3.1}$	-1.95 ± 0.15
LGS-3	2.08	0.94	$7.9^{+3.2}_{-2.4}$	-2.10 ± 0.22
Phoenix	1.29	0.78	…	-1.37 ± 0.2
SM2	0.96	0.43	7.3	−1.76
SM7	10.02	4.50	9.1	−1.17
SM22	2.58	1.34	7.1	−1.03
Shen13-Doc	34.0	34.04	…	…
Shen13-Bashful	115.0	135.52	…	…
BL-1	…	…	…	…
BL-2	…	…	…	…

Note. Column 1: identification of data and models. Column 2: total stellar mass. Column 3: total V luminosity. Column 4: central velocity dispersion. Column 5: metallicity. For galaxies, L_V, σ_v, and [Fe/H] are from McConnachie (2012); the $M_\star$ values are calculated by scaling L_V with the mass–luminosity relation obtained from the SFH solution of each galaxy. $M_\star$ is provided by Sawala et al. (2010) (for SM2, SM7, and SM22) and Shen et al. (2014). For models of Sawala et al. (2010), the L_V are obtained with IAC-star using the model SFHs provided by these authors as input. No data are given for models of Benítez-Llambay et al. (2015), since these authors do not provide them.

The structure of the paper is as follows. Observational data are described in Section 2. The proposed method is explained in Section 3 and applied to a sample of four Local Group dwarf galaxies. SFHs from Section 3 are compared in Section 4 with a representative set of state-of-the-art theoretical models of galaxy formation. The results are discussed in Section 5, together with the main conclusions. As with the previous LCID papers, cosmological parameters of $H_0 = 70.5\,\mathrm{km\,s^{-1}\,Mpc^{-1}}$, $\Omega_m = 0.274$, and a flat universe with $\Omega_\Lambda = 1 - \Omega_m$ are assumed (Komatsu et al. 2009).

2. DATA SELECTION

For this work, regarding the observational material, we have used the SFHs of the galaxies Cetus (Monelli et al. 2010b), Tucana (Monelli et al. 2010a), LGS-3 (Hidalgo et al. 2011), and Phoenix (Hidalgo et al. 2009), obtained by the LCID collaboration. Data were obtained with the ACS and WFPC2 on board the *Hubble Space Telescope*. The SFHs used in this paper were derived using the IAC method, based on the suite of codes IAC-star/IAC-pop/MinnIAC (Aparicio & Gallart 2004; Aparicio & Hidalgo 2009; Hidalgo et al. 2011). For a more detailed analysis, we have divided the three galaxies with larger field coverages—Cetus, Tucana, and LGS-3—into two regions: an inner one, within one scale length from the center, and an outer one, located beyond two scale lengths.

The properties of the galaxies are summarized in Table 1. The total mass in stellar objects ($M_\star$), V luminosity (L_V), velocity dispersion (σ_v), and metallicity ([Fe/H]) are given. L_V, σ_v, and [Fe/H] are from McConnachie (2012). The $M_\star$ values are calculated by scaling L_V with the mass–luminosity relation obtained from the SFH solution of each galaxy. The L_V values range from 0.5×10^6 to $2.6 \times 10^6 L_\odot$, bracketing the limiting value obtained by Bovill & Ricotti (2011a, 2011b) for galaxies likely to be true fossils.

3. IMPROVING TIME RESOLUTION OF THE SFH AT OLD AGES

Robust SFHs are derived from the CMDs of resolved stellar populations, but they are still affected by several sources of uncertainty that limit time resolution. In short, these sources are of three kinds: (1) those affecting data, (2) those linked to physical properties, and (3) those inherent to the methodology used to derive the SFH. Limitations of the first kind are related to photon counting statistics, defective flat-field corrections, or sampling of the point-spread function, among others. Sources of the second kind are mainly distance to the object (contributing to blending and crowding), background and foreground contamination, and differential reddening. The term *observational effects* has often been used by our team to refer to these two kinds combined (see, e.g., Aparicio & Hidalgo 2009) and we will adopt it here from now on. They result in limiting the photometry depth and completeness, which in turn vary with stellar colors and magnitudes. They are modeled (e.g., with artificial star tests) and accounted for when synthetic populations are computed. Effects of the third kind refer to the robustness of the method and include the accuracy of the stellar evolution libraries from which synthetic populations are simulated as well as the way in which the best solution is reached. Other items closely related to the physics of the problem, such as the age–metallicity degeneracy in the CMD, are also involved. All these effects combined result in limitations on time resolution and inaccuracies in age in the final SFH solutions (Aparicio et al. 1997; Aparicio & Hidalgo 2009; Hidalgo et al. 2011).

To derive the SFH from the CMD of a resolved stellar population one makes a reliable simulation of observational effects (sources (1) and (2) above) in the CMD of one or several synthetic stellar populations. These CMDs are in turn compared with the observational CMD to obtain the SFH (see, e.g., Aparicio & Hidalgo 2009; Hidalgo et al. 2011, and references therein). Aparicio & Hidalgo (2009) and Hidalgo et al. (2011) made an analysis of the effects of this process on the time resolution. To a good approximation it can be assumed that, taken together, the effects on the SFH are similar to a temporal shift plus a convolution with a Gaussian function, $G_{\rm obs}$. It should be noticed that average ages of older populations tend to be biased to younger values. This is mainly the effect of the time limit imposed by the method, which does not allow ages older than the age of the universe in the solution.

The function $G_{\rm obs}$ can be obtained according to the following recipe (see Hidalgo et al. 2011). First, a single-burst stellar population with no age dispersion (or a very small one) is computed with the age at which $G_{\rm obs}$ is sought. Second, the observational effects obtained for the galaxy in the artificial star tests are simulated. Third, the SFH of this synthetic population is derived. The result can be taken as $G_{\rm obs}$.

The function $G_{\rm obs}$ can be used to partially remove the observational effects from the SFH derived for a galaxy. To do so, one can proceed parametrically. We do this by (i) computing a large number of model SFHs of given shape, peak, and duration, (ii) convolving them with $G_{\rm obs}$, and (iii) selecting those producing results compatible with the observationally derived SFH. The result of this inverse procedure is not the real, error-free SFH. The problem we are facing is in fact one of a tradeoff between bias and variance (see, e.g., Hastie et al. 2009). Our objective is to remove bias, but the intrinsic

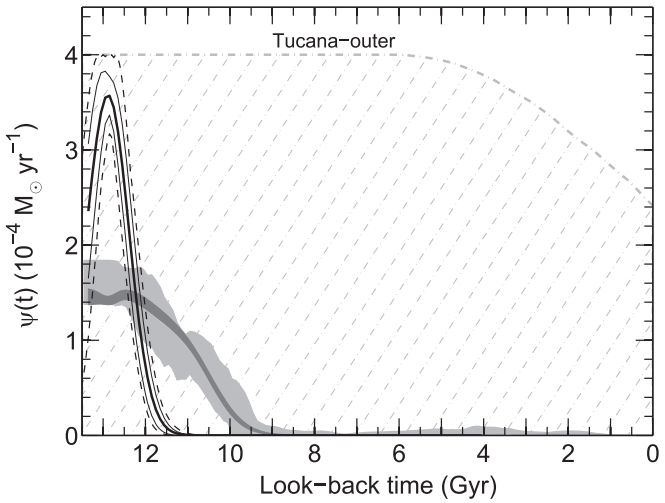

Figure 1. Summary of the models used and the good ones selected for the case of the Tucana-outer field. The gray dashed area shows the envelope of all the used models (about 10^6). The light gray region shows the SFH of the galaxy including the estimate of the 1σ error interval. The dark gray region shows the average of convolved SFHs compatible with empirical results. Its width shows the 1σ dispersion. The thick black line shows the average of the good trial models. Thin black lines show the 1σ dispersion, while thin dashed lines are the envelope of all the good trial models.

variance of the problem remains. Nevertheless it provides a better SFH for comparing to the theoretical models of galaxy formation. This is especially true for the oldest ages, where the limitations on temporal resolution are greatest.

Specifically, we proceed as follows for each observed galaxy field. First, we obtain $G_{\rm obs}$ functions for a range of input ages from 5.0 to 13.0 Gyr and we select the one whose resulting peak age is closest to the peak age of the galaxy SFH. Input ages of the selected $G_{\rm obs}$ functions range from 11.0 (inner LGS-3 field) to 13.0 Gyr (outer Cetus and Tucana fields). Second, we have computed a large number of SFHs shaped according to Gaussian functions of amplitude $y_{\rm G}$, mean age $\tau_{\rm G}$, and standard deviation $\sigma_{\rm G}$. We will refer to these trial model SFHs simply as *trial models*. Values of $\tau_{\rm G}$ have been sampled from 6.0 to 13.5 Gyr in steps of 0.1 Gyr. In turn, $\sigma_{\rm G}$ has been sampled from 0.1 to 6 Gyr in steps of 0.1 Gyr and with the additional criterion that the resulting functions are truncated for age larger than 13.5 Gyr. Trial models include a simple but realistic simulation of the metallicity distribution of the real galaxy for the model age. For this, a gaussian metallicity distribution is used. The mean metallicity is the metallicity observationally obtained for the galaxy at age $\tau_{\rm G}$ and the standard deviation is the metallicity dispersion obtained for the galaxy and the same age. Each trial model shape has been computed a total of 201 times, each one with a different value of $y_{\rm G}$. A total of about 10^6 trial models have been computed for each galaxy field.

In the third step, each trial model has been convolved with the selected $G_{\rm obs}$ function. We will refer by *convolved models* to the results of these convolutions. The fourth step has been to select all the convolved models that are compatible with the SFH obtained for the galaxy field within the error intervals of the latter, including its integral. To apply this criterion, only the age interval $10.0 \leqslant$ age $\leqslant 13.2$ Gyr has been considered. The final step has been to average all the compatible convolved models and, in turn, all the trial models originating them.

Figure 1 shows a summary of the models, including the ones selected for the case of the outer field of the Tucana galaxy.

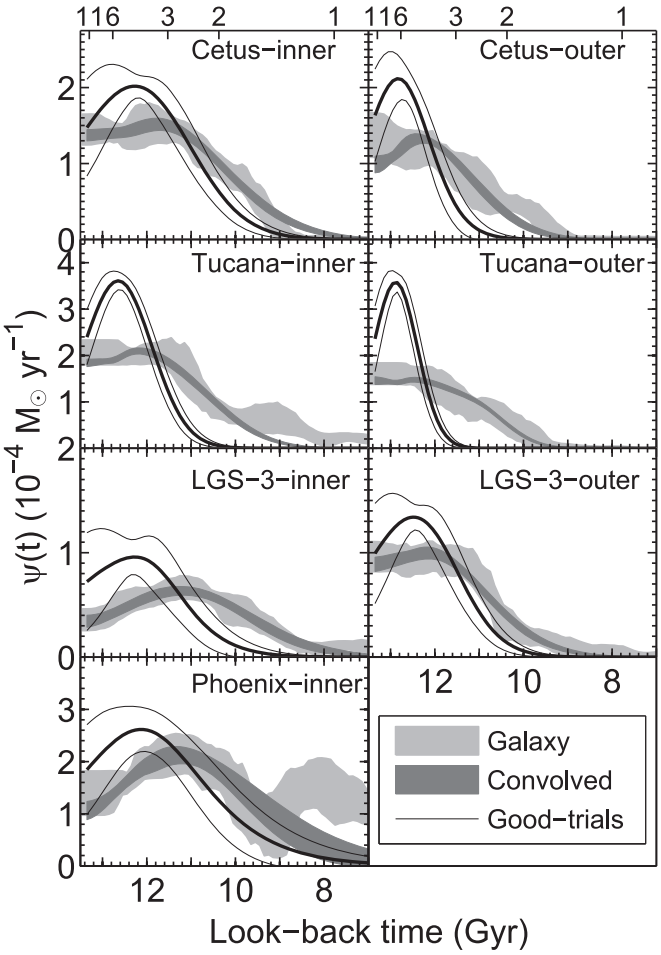

Figure 2. SFHs of the galaxy sample compared with good models. Inner and outer regions are shown for Cetus, Tucana, and LGS-3 while only the inner region is considered for Phoenix. Light gray regions show the SFHs of galaxies, including the estimate of the 1σ error interval. Dark gray regions show the average of convolved models compatible with empirical results. The widths of these regions show the 1σ dispersion. Thick black lines show the average of the good trial models. Thin black lines show the 1σ dispersions.

General results are given in Figure 2, which shows that, except for the case of Phoenix, the average of the *good* trial models peaks at older ages and is narrower than the convolved models or the observational SFHs. Following this, the averages of the good trial models will be used to make direct comparisons to theoretical models of galaxy formation.

The Gaussian functions used above are clearly a simplified representation of the SFH. They are not expected to reproduce extended SFHs or those in which recursive bursts of star formation are going on for an extended period of time. Indeed, Figure 2 shows that intermediate ages for Phoenix are not well reproduced. Nonetheless this can still be a good approximation for old stellar populations, which is the purpose of this exercise. To check for the dependence of the solutions on the shape of the trial model, we have repeated the same experiments using triangular and step functions in turn. In all the cases results are similar and do not significantly change the conclusions of our work.

Since we are interested here in the fraction of stars formed before a given time, it is better to use the cumulative SFH. We define it as $\Psi(t) = \int_T^t \psi(t')dt'$, where $T = 13.5$ Gyr is the age assumed for the onset of star formation and $\psi(t)$ is the star

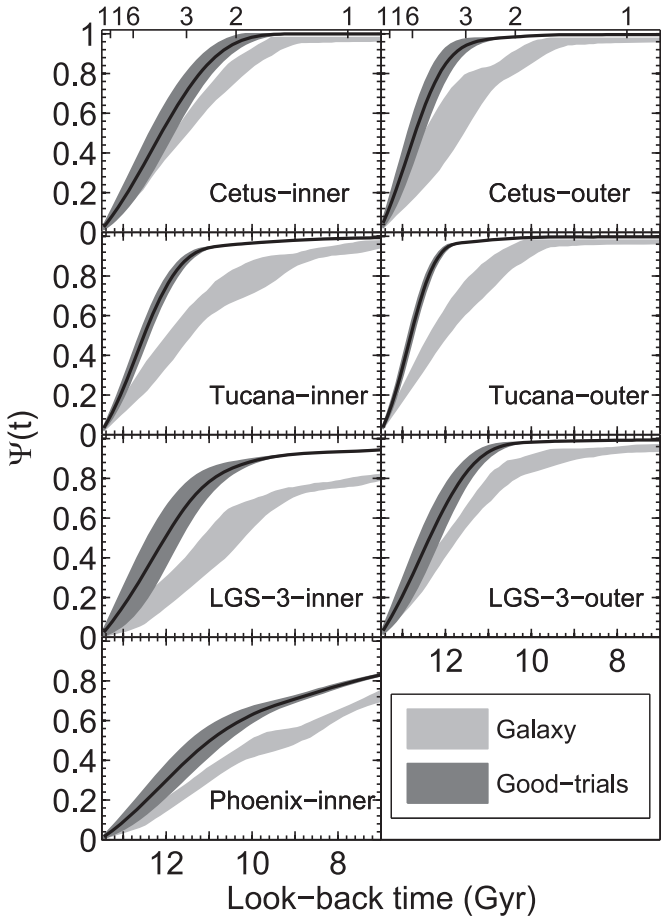

Figure 3. Cumulative SFHs for each galaxy field. Light gray areas show the cumulative SFHs derived from observations. Dark gray areas show the same for the average of the good trial models. See the main text for details.

formation rate. Figure 3 shows the cumulative SFHs observed and for the good trial model for all the galaxy fields. The latter is the information needed to make a direct comparison with theoretical models of galaxy formation.

4. COMPARISON WITH PREDICTIONS FROM THEORETICAL MODELS OF GALAXY FORMATION

In Figure 4 the average of the good trial models of the galaxies is compared with a few representative theoretical models of galaxy formation, namely models 2, 7, and 22 by Sawala et al. (2010), model Doc by Shen et al. (2014), and two models by Benítez-Llambay et al. (2015) representative of old and old+intermediate-age dwarf galaxies. The latter are those given by the authors by the green curves in their Figure 5.

Sawala et al. (2010) have presented high-resolution hydrodynamical simulations of the formation and evolution of isolated dwarf galaxies including the most relevant physical effects, namely, metal-dependent cooling, star formation, feedback from supernovae (SNe) II and Ia, UV background radiation, and internal self-shielding. Models 2 and 7 include UV background radiation and internal self-shielding together with SNe feedback. Model 22 includes only SNe feedback, i.e., it is representative of the case in which UV background radiation has no effect on the SFH.

Shen et al. (2014) have carried out fully cosmological, very high-resolution, ΛCDM simulations of a set of field dwarf

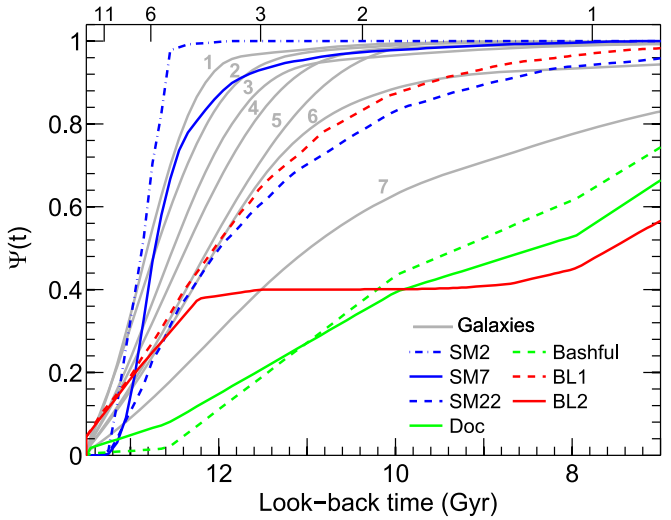

Figure 4. Averages of the good trial models in each galaxy field (plotted by thick black lines in Figure 3) compared with the same for a number of theoretical models of galaxy formation. Numbers in the figure correspond to 1: Tucana-outer, 2: Cetus-outer, 3: Tucana-inner, 4: LGS-3-outer, 5: Cetus-inner, 6: LGS-3-outer, and 7: Phoenix-inner. Regarding the models, SM2, SM7, and SM22 are respectively models 2, 7 and 22 by Sawala et al. (2010). Models Doc and Bashful are by Shen et al. (2014). Models BL-1 and BL-2 are models 1 and 2 by Benítez-Llambay et al. (2015).

galaxies. Model Doc corresponds to a virial mass of $M_{\rm vir} = 1.16 \times 10^{10} M_{\odot}$. Finally, Benítez-Llambay et al. (2015) have used the cosmological hydrodynamical simulation of the Local Group carried out as part of the CLUES project. In all cases, the reader is referred to the source papers for details.

Some relevant properties of the model galaxies are summarized in Table 1. The total mass in stellar objects ($M_{\star}$), V luminosity (L_V), velocity dispersion (σ_v), and metallicity ([Fe/H]) are given. $M_{\star}$ is provided by Sawala et al. (2010) and Shen et al. (2014). Regarding L_V, the values given by Shen et al. (2014) are listed for their models. For the models of Sawala et al. (2010), the L_V are obtained with IAC-star using the model SFHs provided by these authors as input. No data are given for the models of Benítez-Llambay et al. (2015), since these authors do not provide them.

Figure 4 shows that the average of the cumulative good trial models of Cetus, Tucana, and LGS-3 lay between models SM2 and SM7 (both including reionization), on the one side, and models SM22 (without reionization) and BL-1 (average of their oldest models), on the other side. Furthermore, the outer parts of Cetus and Tucana show a reasonable correspondence with SM7, indicating that reionization could have played a role in quenching the star formation in those regions. However, according to this figure, the inner regions of both galaxies plus LGS-3 (inner and outer) and Phoenix seem difficult to reconcile with the models of Sawala et al. (2010) with reionization. A good correspondence exists between the inner region of LGS-3 and models BL-1 and SM22, while no good match is found for Phoenix with any of the models considered here. Finally, models BL-2, Doc, and Bashful are, by far, too young to reproduce any of the observed galaxies and are likely to be more suitable for much younger galaxies, like IC-1613 (see Skillman et al. 2014).

Bovill & Ricotti (2011b) have defined true fossil galaxies as those having formed all or most of their stars before the reionization era, at $z = 6$. They used the cumulative fraction of

Table 2
Age for $\Psi(t) = 0.7$ and the $\Psi(t)$ Value for $z = 6$

Galaxy Field	Age for $\Psi(t)$=0.7 Observational	$\Psi(t)$ at $z = 6$ Observational	Age for $\Psi(t) = 0.7$ Good Trials	$\Psi(t)$ at $z = 6$ Good Trials
Cetus-inner	$10.9^{+0.2}_{-0.2}$	$0.22^{+0.03}_{-0.07}$	$11.6^{+0.3}_{-0.4}$	$0.25^{+0.18}_{-0.19}$
Cetus-outer	$11.3^{+0.3}_{-0.6}$	$0.28^{+0.09}_{-0.13}$	$12.4^{+0.2}_{-0.3}$	$0.46^{+0.24}_{-0.12}$
Tucana-inner	$10.8^{+0.7}_{-0.3}$	$0.21^{+0.05}_{-0.06}$	$12.1^{+0.1}_{-0.1}$	$0.36^{+0.12}_{-0.06}$
Tucana-outer	$11.5^{+0.4}_{-0.3}$	$0.29^{+0.03}_{-0.06}$	$12.6^{+0.0}_{-0.1}$	$0.53^{+0.11}_{-0.05}$
LGS-3-inner	$9.4^{+0.3}_{-0.5}$	$0.10^{+0.04}_{-0.06}$	$11.4^{+0.4}_{-0.4}$	$0.23^{+0.25}_{-0.13}$
LGS-3-outer	$11.2^{+0.3}_{-0.2}$	$0.23^{+0.05}_{-0.06}$	$11.9^{+0.3}_{-0.2}$	$0.31^{+0.22}_{-0.11}$
Phoenix-inner	$7.3^{+0.3}_{-0.2}$	$0.08^{-0.03}_{-0.03}$	$9.1^{+0.3}_{-0.2}$	$0.13^{+0.05}_{-0.11}$
SM2	…	…	12.8	0.98
SM7	…	…	12.5	0.67
SM22	…	…	11.0	0.31
Shen13-Doc	…	…	6.7	0.08
Shen13-Bashful	…	…	7.3	0.02
BL-1	…	…	11.2	0.34
BL-2	…	…	5.8	0.30

Note. Column 1: data source: observational inner or outer field for each galaxy or model; observational source: Hidalgo et al. (2013); model sources: Sawala et al. (2010), Shen et al. (2014), and Benítez-Llambay et al. (2015). Column 2: age at which the cumulative SFH $\Psi(t)$ reaches 70%. Column 3: value of $\Psi(t)$ corresponding to $z = 6$. Values listed in columns 2 and 3 have been obtained from Figure 3.

star formation produced before reionization as a test to distinguish true fossil galaxies from non-fossils, defining the former as those having produced at least 70% of their stars at $z = 6$, which, for the cosmological parameters adopted here (see above), corresponds to approximately 12.8 Gyr ago. Table 2 gives, for each galaxy field and model, the age at which $\Psi(t) = 0.7$ and the value of $\Psi(t)$ for redshift $z = 6$. Columns 2 and 3 list the values corresponding to the observed SFHs. Columns 4 and 5 give those corresponding to the average of the good trial models. Errors have been obtained from the error bands shown in Figure 3.

Two main conclusions can be obtained from Table 2. First, the age for which the cumulative SFH, $\Psi(t)$, reaches 70% is increased by observational effects by ∼1.25 Gyr on average, while the value of $\Psi(t)$ at $z = 6$ is increased by a factor of ∼1.65 on average, although it can be larger than two in some cases. This shows that working with the average of good trial models is useful if the earliest evolution of dwarf galaxies is sought. Second, taken at face value, none of the four galaxies analyzed here fulfills the criterion by Bovill & Ricotti (2011b) of having $\Psi(t) \geqslant 0.7$ at $z = 6$, necessary for them to be considered true fossils from the pre-reionization era, although the outer regions of Cetus and Tucana might marginally qualify, within a 2σ error interval. In addition, Bovill & Ricotti (2011b) also concluded that galaxies with $L_V > 10^6\, L_\odot$ are unlikely to be true fossils, while those with $L_V < 10^6\, L_\odot$ remain reasonable candidates to be fossils of the first generation of galaxies. However, three out of the four galaxies considered here have $L_V \leqslant 10^6 L_\odot$ (Tucana, LGS-3, and Phoenix) and are not true fossils.

5. SUMMARY AND CONCLUSIONS

In summary, we have presented a method to address the limitations of the temporal resolution of the early SFHs of galaxies derived from deep CMD modeling. We have applied the method to the analysis of the duration of the early star formation activity in a sample of Local Group dwarf galaxies with the purpose of testing whether or not they are true fossils of the pre-reionization era. For a study of this kind to be accurate, the affects of limited time resolution need to be accounted for. For testing for fossils, using SFHs derived directly from deep CMD modeling may produce biased results due to limited time resolution. We have shown elsewhere (Hidalgo et al. 2011) that the SFH derived for a synthetic stellar population of single age and metallicity can be simulated by a Gaussian whose standard deviation depends on age ($G_{\rm obs}$). The method presented here consists in computing a large number of stellar populations with Gaussian SFHs and metallicity distribution similar to that obtained for the galaxy for the same age interval (that we call *trial models*; about 10^6 per galaxy in this case) of varying mean, standard deviation, and amplitude, and selecting all those that, convolved with $G_{\rm obs}$, produce results compatible with the optimal SFH derived directly from observations. The average of the good trial models is an improved approach to the real SFH of the galaxy at the very earliest times. In general, the ages of the averages of the good trial models are about ∼1.25 Gyr older than the optimal SFH solutions for the case of predominantly old galaxies.

We have applied our method to four Local Group dwarfs—Cetus, Tucana, LGS-3, and Phoenix—and we have compared our results with predictions made by a number of recent cosmological hydrodynamical simulations for the formation and evolution of dwarf galaxies. A relatively sharp exhaustion of the star formation is necessary at an early epoch, close to $z = 6$, to account for the SFH obtained for the outer region of Tucana and Cetus. The inner parts of both galaxies, as well as LGS-3 and, more clearly, Phoenix, are compatible with models predicting more extended star formation activity for dwarf galaxies. However, none of the galaxies and fields studied here, except perhaps the outer regions of Cetus and Tucana, fulfills the criterion necessary for them to be considered as fossil remnants of the pre-reionization era. As a cautionary note, at present, it cannot be excluded that Cetus and Tucana were affected by environmental effects to some extent. Their distances to the two massive spirals of the Local Group, while placing them outside the virial radius of either today, are still small enough to admit scenarios in which these galaxies are on nearly radial orbits, and they may have already had a close pericenter passage with their host (Kazantzidis et al. 2011). If

they are bound satellites, their relatively large velocity dispersion, $\sigma_v \sim 15\,\mathrm{km\,s^{-1}}$ (see Table 1), would make them comparable to the brightest dSph satellites such as Fornax, and implies that their halos could have been much more massive before tides began to prune them substantially. If this were the case, it would be likely that their halo mass before infall was high enough to place them clearly above the threshold mass for reionization to play a role, strengthening further the conclusion that they cannot be reionization fossils.

The authors thank the anonymous referee for her/his comments and suggestions, which have helped to improve the clarity of the paper. This work has been funded by the Economy and Competitiveness Ministry of the Kingdom of Spain (grants AYA2010-16717 and AYA2013-42781-P) and by the Instituto de Astrofísica de Canarias (grant P3/94).

REFERENCES

Aparicio, A., & Gallart, C. 2004, AJ, 128, 1465
Aparicio, A., Gallart, C., & Bertelli, G. 1997, AJ, 114, 680
Aparicio, A., & Hidalgo, S. L. 2009, AJ, 138, 558
Becker, G. D., Bolton, J. S., Madau, P., et al. 2015, MNRAS, 447, 3402
Becker, R. H., Fan, X., White, R. L., et al. 2001, AJ, 122, 2850
Benítez-Llambay, A., Navarro, J. F., Abadi, M. G., et al. 2015, MNRAS, 450, 4207
Bovill, & Ricotti 2011a, ApJ, 741, 17
Bovill, & Ricotti 2011b, ApJ, 741, 18
Bullock, J. S., Kravtsov, A. V., & Weinberg, D. H. 2000, ApJ, 539, 517
Gnedin, N. Y. 2000, ApJ, 542, 535
Gnedin, N. Y., & Kravtsov, A. V. 2006, ApJ, 645, 1054
Grebel, E. K., & Gallagher, J. S., III 2004, ApJL, 610, L89
Hastie, T., Tibshirani, R., & Friedman, J. 2009, The Elements of Statistical Learning (New York: Springer)
Hidalgo, S. L., Aparicio, A., Martínez-Delgado, D., & Gallart, C. 2009, ApJ, 705, 704
Hidalgo, S. L., Aparicio, A., Skillman, E., et al. 2011, ApJ, 730, 14
Hidalgo, S. L., Monelli, M., Aparicio, A., et al. 2013, ApJ, 778, 103
Iliev, I. T., Moore, B., Gottlöber, S., et al. 2011, MNRAS, 413, 2093
Kauffmann, G., White, S. D. M., & Guiderdoni, B. 1993, MNRAS, 264, 201
Kazantzidis, S., Łokas, E. L., Callegari, S., et al. 2011, ApJ, 726, 98
Kazantzidis, S., Mayer, L., Mastropietro, C., et al. 2004, ApJ, 608, 663
Klypin, A., Kravtsov, A. V., Valenzuela, O., & Prada, F. 1999, ApJ, 522, 82
Komatsu, E., Dunkley, J., Nolta, M. R., et al. 2009, ApJS, 180, 330
Kravtsov, A. V., Gnedin, O. Y., & Klypin, A. A. 2004, ApJ, 609, 482
Loeb, A., & Barkana, R. 2001, ARA&A, 39, 19
Mac Low, M.-M., & Ferrara, A. 1999, ApJ, 513, 142
Mayer, L. 2010, AdAst, 2010, 278434
Mayer, L., Kazantzidis, S., Mastropietro, & Wadsley, C. 2007, Natur, 445, 738
McConnachie, A. W. 2012, AJ, 144, 4
Monelli, M., Gallart, C., Hidalgo, S. L., et al. 2010a, ApJ, 722, 1864
Monelli, M., Hidalgo, S. L., Stetson, P. B., et al. 2010b, ApJ, 720, 1225
Moore, B., Ghigna, S., Governato, F., et al. 1999, ApJL, 524, L19
Peñarrubia, J., Navarro, J. F., & McConnachie, A. W. 2008, ApJ, 673, 226
Ricotti, M., & Gnedin, N. Y. 2005, ApJ, 629, 259
Sawala, T., Scannapieco, C., Maio, U., & White, S. 2010, MNRAS, 402, 1599
Schaye, J. 2001, ApJL, 562, L95
Shen, S., Madau, P., Conroy, C., et al. 2014, ApJ, 792, 99
Skillman, E. D., Hidalgo, S. L., Weisz, D. R., et al. 2014, AJ, 786, 44
Sobacchi, E., & Mesinger, A. 2015, MNRAS, 453, 1843
Spitler, L. R., Romanowsky, A. J., Diemand, J., et al. 2012, MNRAS, 423, 2177
Susa, H., & Umemura, M. 2004, ApJL, 610, L5
Tomozeiu, M., Mayer, L., & Quinn, T. 2015, ApJ, 818, 193
Weisz, D. R., Dolphin, A. E., Skillman, E. D., et al. 2014a, ApJ, 789, 147
Weisz, D. R., Dolphin, A. E., Skillman, E. D., et al. 2014b, ApJ, 789, 148